

Reprint from

“PLASMA PHYSICS
AND CONTROLLED
NUCLEAR FUSION RESEARCH 1982”

VOL. III

INTERNATIONAL ATOMIC ENERGY AGENCY
VIENNA, 1983

CONFINEMENT IN TOROIDAL SYSTEMS WITH PARTIALLY DESTROYED MAGNETIC SURFACES

R.B. WHITE, A.H. BOOZER, R. GOLDSTON,
R. HAY, J. ALBERT, C.F.F. KARNEY
Plasma Physics Laboratory,
Princeton University,
Princeton, New Jersey,
United States of America

Abstract

CONFINEMENT IN TOROIDAL SYSTEMS WITH PARTIALLY DESTROYED MAGNETIC SURFACES.

A Hamiltonian formulation of the guiding centre drift equations valid for stochastic fields is given. Modification of neoclassical transport due to imperfect magnetic surfaces is investigated numerically. For banana-trapped particles a discrete map representation is given for the orbits and used to study loss of banana-trapped α -particles due to field ripple.

I. Hamiltonian Formulation of the Guiding Center Drift Equations

Recently developed methods of analysis are providing new insight into problems involving nonlinear equations of motion which, although deterministic, lead to apparently chaotic behavior. This subject is of immediate importance for magnetic fusion research, where small asymmetries in magnetic fields can lead to stochastic particle orbits and poor confinement. The calculation of the orbits of charged particles in given electric and magnetic fields is one of the oldest problems in plasma physics. To facilitate the numerical evaluation of long time confinement parameters such as diffusion rates, an average must be made over the rapid gyro motion of the particles. The resulting guiding center equations have played an important role in plasma physics since their inception [1-7].

It is particularly convenient to use magnetic coordinates for confinement studies. These coordinates, in addition to defining the surfaces across which diffusion is relevant, separate fast and slow time scales related to motion along and across the field. As we will show, in a Hamiltonian formalism they are also intimately related to the canonical variables for the guiding center motion. Of course a stochastic field has no such coordinates, but the systems of interest for confinement studies are necessarily

only small perturbations of systems with good magnetic surfaces. We therefore assume the existence of a nearby field, \vec{B} with good surfaces.

We will use two representations for \vec{B} , the familiar Clebsch representation and a covariant representation:

$$\vec{B} = \vec{\nabla}\psi \times \vec{\nabla}\zeta = \Lambda(\vec{\nabla}\chi + \beta^* \nabla\psi) \quad (1)$$

The variable ψ labels the flux surfaces, and ζ is a measure of the angle around a flux surface across the field. The quantity Λ is the permeability, defined by the condition $\vec{\nabla}\psi \cdot \vec{\nabla} \times (\vec{B}/\Lambda) = 0$. For scalar pressure equilibria $\Lambda = 1$, and Grad [8] has shown that for tensor pressure equilibria $1/\Lambda = 1 + (P_{\perp} - P_{\parallel})/B^2$. The quantity β^* is related to the parallel current and pressure through $\vec{B} \cdot \vec{j} = -B^2 \partial\beta^*/\partial\zeta$, $\partial P/\partial\psi = B^2 \partial\beta^*/\partial\chi$, and χ measures the distance along a field line. Given any explicit representation of \vec{B} in toroidal coordinates r, θ, ϕ , the magnetic coordinates can be found by comparison with Eq. (1). Consider a torus of aspect ratio $\epsilon^{-1} = R/a$, with R and a the major and minor radii. The simplest non-trivial toroidal system is given by the truncation to first order in ϵ of a zero pressure equilibrium [9]

$$\vec{B} = \frac{r}{q(r)} \vec{\nabla}\phi \times \vec{\nabla}r + R\vec{\nabla}\phi \quad (2)$$

where we have normalized \vec{B} to its value on axis. The coordinate r labels the magnetic surface so we can take $\psi = r^2/2$. We then find $\zeta = \theta - \phi/q - r/R \sin\theta$, $\chi = \phi/\epsilon + r^2\theta/qR$, and $\beta^* = -(\theta/rR)(d/dr)(r^2/q)$. These expressions are readily evaluated to higher order in ϵ using higher order expressions for \vec{B} [9]. The analysis of transport in a finite pressure plasma using the higher order formalism will be the subject of a future publication.

We assume that the exact magnetic field of interest can be represented through $\vec{B} = \vec{B} + \delta\vec{B}$ where \vec{B} is a field which can be described by Eq. (1) and $\delta\vec{B}$ represents the effect of magnetic field coils, plasma modes, etc. As has been shown [10], one component of $\delta\vec{B}$, namely $\delta\vec{B} \cdot \vec{\nabla}\psi$, dominates the structure of the perturbed surfaces. Other components of $\delta\vec{B}$ contribute only non-resonant distortions of the equilibrium and are unimportant. We represent this component of $\delta\vec{B}$ exactly through $\delta\vec{B} = \vec{\nabla} \times \alpha\vec{B}$ with α a general function of position. If α is represented through its Fourier series

$$\alpha = \sum_{m,n} \alpha_{nm}(r) \cos(n\phi - m\theta - \delta_{mn}) \quad (3)$$

we find that α changes the topology of \vec{B} at rational surfaces $q = m/n$, producing islands of width

$$\left(\frac{\delta r}{r}\right) = \left| \frac{4q^2}{rq'} \frac{B_\phi}{B_\theta} \frac{\alpha_{nm}}{r} \right|^{1/2} \quad (4)$$

Typically, $\alpha/r \sim 10^{-5}$ produces islands of width $\delta r/r \sim 10^{-2}$, so that very small α is sufficient to represent quite stochastic fields. In terms of particle orbits, other components of $\delta\vec{B}$ affect only the perpendicular drift velocity which is also proportional to the gyro radius, whereas topology changes, proportional to $\alpha^{1/2}$, modify the parallel motion and are clearly dominant for α much smaller than the system size.

A convenient form of the guiding center drift, first formulated by Morozov and Solovév [11] and modified by Boozer [5] and Littlejohn [6], is given by

$$\vec{v} = \frac{v_{\parallel}}{B} \frac{1}{1 + \rho_{\parallel} \hat{b} \cdot \nabla \times \hat{b}} [\vec{B} + \nabla \times \rho_{\parallel} \vec{B}] \quad (5)$$

where $\rho_{\parallel} = v_{\parallel} / \omega_c = [2E - 2\mu B - 2\Phi]^{1/2} / B$ is the "parallel gyro radius", $\hat{b} = \vec{B} / B$, and the gradient operator in Eq. (5) acts on ρ_{\parallel} with E, μ fixed. Here and in the following we use units of time given by $\omega_0 = eB_0 / mc$ and lengths given by the minor radius.

The Hamiltonian character of \vec{v} can be demonstrated by finding the canonical variables, closely related to the magnetic coordinates [12]. First introduce the perturbation $\vec{B} \rightarrow \vec{B} + \nabla \times \alpha \vec{B}$, in Eq. (5). Neglecting terms of order $\rho_{\parallel} \alpha$, \vec{v} is then given by Eq. (5) with ρ_{\parallel} replaced by $\rho_c = \rho_{\parallel} + \alpha$. The rate of change of the magnetic coordinates and of ρ_c , $\dot{\psi} = \vec{v} \cdot \nabla \psi$, $\dot{\rho}_c = v_{\parallel} \nabla_{\parallel} \rho_c$ etc. can be expressed as a linear combination of the terms $\partial H / \partial \psi$, $\partial H / \partial \zeta$, $\partial H / \partial \chi$, $\partial H / \partial \rho_c$ where the Hamiltonian is

$$H = \frac{1}{2} B^2 \rho_{\parallel}^2 + \mu B + \Phi \quad (6)$$

Transformation to the variable $\theta = \zeta - \beta^* \rho_c$ then puts these equations into canonical form and gives for the drift equations

$$\dot{\chi} = \frac{\partial H}{\partial \rho_c}, \quad \dot{\rho}_c = -\frac{\partial H}{\partial \chi}, \quad \dot{\theta}_c = \frac{\partial H}{\partial \psi}, \quad \dot{\psi} = -\frac{\partial H}{\partial \theta_c} \quad (7)$$

One of the advantages of the Hamiltonian formalism is that simplifications and idealizations can be made in the functional

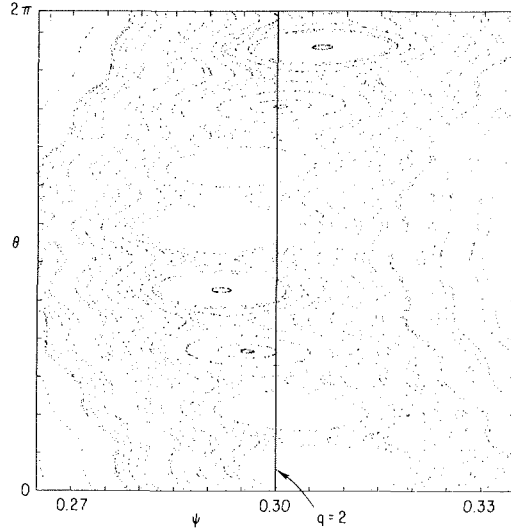


FIG.1. Poincaré plot made with 1 keV ions, with $\mu = 0$. A single $m = 8, n = 4$ mode is present. The ions follow the magnetic islands as well as executing large-scale drift motion.

form of the magnetic field without sacrificing exact energy conservation and the Liouville theorem. For example the use of the first-order model given by Eq. (2) gives, to order ϵ , $B = 1 - \epsilon \cos \theta$ with $\theta = \zeta + \epsilon \chi / q(r)$. Further we can take $\theta_c = \zeta$, since β^* produces a correction to B of order $\epsilon^2 \rho_{\parallel}$. The Hamiltonian then gives a set of drift orbit equations which, although idealized, exactly conserve energy and satisfy the Liouville theorem.

II. Modification of Neoclassical Transport

The first-order (in ϵ) model Eq. (2) has been used to produce Poincaré maps for magnetic fields as well as for drift orbits, and to investigate the modification of neoclassical diffusion due to the destruction of magnetic surfaces. Shown in Fig. 1 is a Poincaré map obtained using 1 keV ions with $\mu = 0$ and a perturbation α of magnitude $\alpha/a = 10^{-5}$ with $m = 8, n = 4$. The island size for the ion orbits is the same as those for the magnetic field, but in addition the ion orbits are displaced from the $q = 2$ surface by drift motion. This indicates that, at least for passing particles, the stochastic threshold for the drift orbits corresponds to that for the magnetic field itself.

To study particle diffusion we have introduced energy-conserving pitch angle scattering. The pitch $\lambda = v_{\parallel} / v$ is changed every time step by

$$\lambda' = \lambda(1 - \nu\tau) \pm [(1 - \lambda^2)\nu\tau]^{1/2} \quad (8)$$

where ν is the collision frequency, τ is the time step with $\nu\tau \ll 1$, and the \pm implies a random sign. This can be shown to give an equivalent Lorentz collision operator [13]. We have studied the modification of neoclassical banana diffusion as a function of the perturbing field amplitude in a simple model consisting of equally spaced modes of equal amplitude [14]. Three qualitatively different regimes exist. Parameterize the magnitude of α in terms of a stochasticity parameter s , with α given by Eq. (3) with $\alpha_{nm} = s$. If $s \ll s_c$, where s_c is the threshold for stochasticity [15] of the exact field \vec{B} , the particles diffuse according to the neoclassical rate [16].^e If $s \lesssim s_c$ a significant fraction of space is filled with magnetic islands, which give rise to enhanced transport much in the way banana orbits contribute to neoclassical diffusion. Diffusion due to a combination of islands and a collision term has been investigated previously [17,18,19], but the results cannot be directly compared because of the quite different particle orbits. Finally, if $s > s_c$ the diffusion is given by the particles streaming along the stochastic field, and can be calculated [20] using the random phase approximation for the modes in α .

Figure 2 shows the obtained diffusion coefficients for 1 keV ions and electrons. We have used a 30 kG field, $a = 30$ cm, and $\epsilon = 1/4$. The q profile was taken to be linear in ψ , ranging from 1.0 on axis to 4.0 at the wall. The modes had $n = 4$ and $m = 7, 8, 9$. A significant modification of the electron neoclassical diffusion rate exists below the stochastic threshold, whereas the ions are relatively unaffected because island-banana diffusion is overshadowed by the large ion neoclassical rate.

Neutrality of the plasma would of course not permit large differences in electron and ion diffusion to occur, but similar modification of electron heat transport is to be expected. We have begun to assess the role of MHD modes on particle confinement. Recent three dimensional non linear resistive MHD simulations of MHD activity during high power neutral beam injection into high temperature plasmas in PDX display a large variety of modes, primarily driven by the sawtooth ($m = 1, n = 1$) oscillation. In Fig. 3 is shown a Poincaré plot of the magnetic field surfaces during a typical discharge. Although the field is somewhat below stochastic threshold in most domains, the abundance

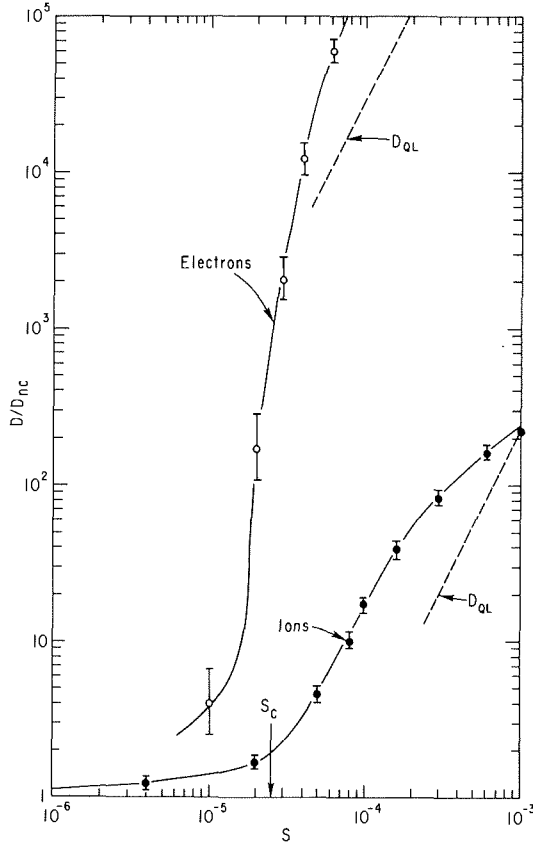


FIG.2. The electron and ion diffusion coefficients, normalized to their neoclassical values, D_{nc} , as a function of the amplitude of the perturbing fields, s . Here $v_e/\omega_e = 1.8 \times 10^{-8}$, $v_i/\omega_i = 10^{-6}$, $a/\rho_e = 12\,000$, and $a/\rho_i = 200$. Also shown are the quasilinear values and the stochastic threshold. The value of D_e at $S = 10^{-5}$ has been changed from that given in Ref.[14] by the development of a more accurate and efficient method of measuring small diffusion rates.

of magnetic islands must be expected to contribute significantly to particle diffusion.

III. Discrete Map Representation of Banana Orbits

A further simplification of the description of particle orbits can be made in the case of banana-trapped particles. In an axisymmetric system the radial drift averages to zero along an orbit. In a non axisymmetric system, however, $v_{||}$ oscillates as a result of the field perturbation, giving rise to an additional oscillating radial excursion. Along most of the trajectory these

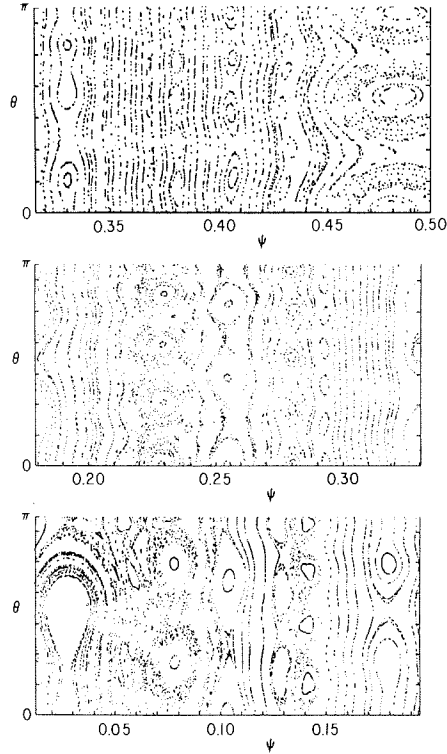


FIG.3. Poincaré plot of the magnetic field in PDX during large-amplitude sawtooth oscillations. The safety factor profile is modelled as $q = 0.82 + 6.6 \psi$. We kept the 30 largest modes of the simulation, with $1 \leq m \leq 12$, $1 \leq n \leq 4$ and amplitudes α_{nm} ranging from 10^{-7} to 10^{-4} , with average amplitude 1.5×10^{-5} .

small excursions are self cancelling, but near the turning points the excursions are largest and do not cancel. Using the model magnetic field, $B = B_0(1 - \epsilon r \cos \theta + \delta \cos N\phi)$, where δ is the local ripple magnitude, one can integrate along unperturbed trajectories analytically to find the displacement after a single bounce, $\Delta(r)$. The toroidal angle between two turning points is $\phi_b = 2q\theta_t$, with $\cos \theta_t = (R_b - R)/r$, and R_b , the bounce radius, is a constant of the motion in order to conserve B at the turning points. Let $\phi_p(r)$ be the amount the banana orbit precesses toroidally while moving between turning points. An area preserving map of the banana orbit motion is given by

$$r_{j+1} = r_j + \Delta(r_{j+1}) \cos(N\phi_j - \pi/4)$$

INTOR
 $1 < q < 3$
 Rounded Profile

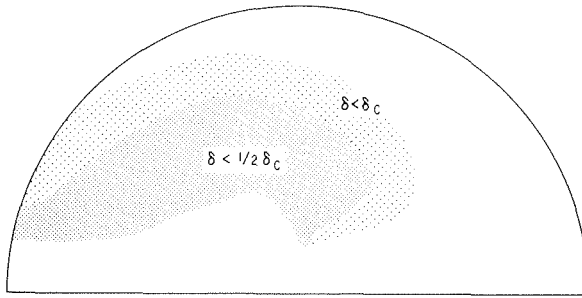


FIG.4. The region of confined banana-trapped α -particles for typical INTOR design parameters, $1 < q < 3$. Particles with banana tips in the shaded region are confined, those in the partially shaded region are marginal, and others are lost.

$$\phi_{j+1} = \phi_j + \phi_b(r_{j+1}) + \phi_p(r_{j+1}) - \Delta'(r_{j+1})\sin(N\phi_j - \pi/4)/N \quad (9)$$

$$r_{j+2} = r_{j+1} + \Delta(r_{j+2})\cos(N\phi_{j+1} + \pi/4)$$

$$\phi_{j+2} = \phi_{j+1} - \phi_b(r_{j+2}) + \phi_p(r_{j+2}) - \Delta'(r_{j+2})\sin(N\phi_{j+1} + \pi/4)/N$$

where the first and third equations must be solved iteratively, and the $\Delta' = d\Delta/dr$ terms are necessary modifications of ϕ at the banana tips in order that the map be area-preserving. The first half of this map represents the changes in r, ϕ evaluated at the lower banana tip, and the second half at the upper banana tip. The local approximation to this map, $\Delta(r) = \text{const}$, has been used previously [21] to investigate the threshold in ripple magnitude for the onset of stochastic banana trajectory motion, and hence particle loss, for fusion-product, banana-trapped α particles. An approximate expression for this threshold is

$$\delta_c \approx [(\pi Nq/\epsilon)^{3/2} \rho q']^{-1} \quad (10)$$

which for typical reactor design parameters gives a limit of 0.3% on δ . In Fig. 4 is shown the extent of stable banana trajectories for typical INTOR parameters. The generalized map, Eq. (9), is appropriate for studying long time transport of banana-trapped particles. The toroidal precession rate ϕ_p can be calculated

using expressions for the toroidal velocity [22] and the bounce-averaged pitch [23]. We find for small ε

$$\phi_p = -\rho_\theta \left\{ q'4 \sqrt{2\varepsilon r} [E - (1-\xi^2/2\varepsilon r)K] + \frac{q}{R} \sqrt{2/\varepsilon r} [2E - K] \right\} \quad (11)$$

where ρ_θ is the poloidal gyro radius, E and K are elliptic functions with argument $\xi^2/2\varepsilon r$, and $\xi = v_\parallel/v$ evaluated at $\theta = 0$.

For collisional effects we use the bounce-averaged collision operator of Cordey [23] to obtain appropriate displacement and diffusion in pitch angle. Integrating over a single bounce time we find, using the notation of Cordey,

$$\langle \Delta \xi \rangle = \frac{2\pi q R \beta v_c^3}{\tau_b v^4 \xi} \left[(1-\xi^2) \langle v/v_\parallel \rangle - \frac{(1+\xi^2)}{\xi^2} \langle v_\parallel/v \rangle \right] \quad (12)$$

where $\langle v/v_\parallel \rangle = \frac{2}{\pi \sqrt{2\varepsilon r}} K$, $\langle v_\parallel/v \rangle = \frac{2\sqrt{2\varepsilon r}}{\pi} [E - (1-\frac{\xi^2}{2\varepsilon r})K]$, and

$$\langle (\Delta \xi)^2 \rangle = \frac{4\pi q R \beta v_c^3}{\tau_b v^4} \left[\frac{(1-\xi^2)}{\xi^2} \langle v_\parallel/v \rangle \right] \quad (13)$$

Taken together the mapping and collision operator constitute a complete Monte-Carlo formalism for studying the banana-kinetic equation in toroidal systems.

ACKNOWLEDGEMENTS

This work was supported by United States Department of Energy Contract No. DE-AC02-76-CH03073.

The authors acknowledge useful discussions with J. Greene, D.A. Monticello, W. Park and K. McGuire.

One of the authors (RBW) is indebted to the Aspen Center for Physics for their hospitality during a visit, where some of this work was completed.

REFERENCES

- [1] H. Alfvén, Ark. Nat. Astron. Fys. 27A 1 (1940)
- [2] C. S. Gardner, Phys. Rev. 115 (1959) 791
- [3] T. G. Northrop, The Adiabatic Motion of Charged Particles, Wiley, New York (1963)
- [4] T. G. Northrop and J. A. Rome, Phys. Fluids 21 (1978) 384
- [5] A. H. Boozer, Phys. Fluids 23 (1980) 904
- [6] R. G. Littlejohn, Phys. Fluids 24 (1981) 1730
- [7] H. Weitzner, Phys. Fluids 24 (1981) 2280
- [8] H. Grad, Proc. Symp. Appl. Math 18 (1967) 162
- [9] J. M. Greene, J. L. Johnson, and K. E. Weimer, Phys. Fluids 14 (1971) 671
- [10] M. N. Rosenbluth, R. Sagdeev, J. B. Taylor, and G. M. Zaslavsky, Nucl. Fus. 6 (1966) 297
- [11] A. I. Morozov and L. S. Solovév in Reviews of Plasma Physics, edited by M. A. Leontovich (Consultants Bureau, New York, 1965) Vol. 2, p. 228
- [12] R. B. White, A. H. Boozer, and Ralph Hay, Phys. Fluids 25 (1982) 575
- [13] A. H. Boozer and G. Kuo-Petravic, Phys. Fluids 24 (1981) 851
- [14] A. H. Boozer and R. B. White, Phys. Rev. Lett. 49 786 (1982)
- [15] V. Chirikov, Phys. Rep. 52 (1979) 263
- [16] M. N. Rosenbluth, R. D. Hazeltine, and F. L. Hinton, Phys. Fluids 15 (1972) 116
- [17] A. B. Rechester and R. B. White, Phys. Rev. Lett. 44 (1980) 1586
- [18] A. B. Rechester, M. N. Rosenbluth, and R. B. White Phys. Rev. 23 (1981) 2664
- [19] C. F. F. Karney, A. B. Rechester, and R. B. White, Physica 4D (1982) 425
- [20] M. N. Rosenbluth, R. Z. Sagdeev, J. B. Taylor, and G. M. Zaslavsky, Nucl. Fus. 6 (1966) 297
- [21] R. J. Goldston, R. B. White, and A. H. Boozer, Phys. Rev. Lett. 47 (1981) 647
- [22] B. B. Kadomtsev and O. P. Pogutse, Nucl. Fus. 11 (1971) 67
- [23] J. G. Cordey, Nucl. Fus. 16 (1976) 499

DISCUSSION

B. McNAMARA: Have you investigated the effect of this diffusion on the ambipolar potential and the effect of the potential on the orbits and the diffusion?

R.B. WHITE: The ambipolar potential is included in the formalism, but

numerical results regarding the effect of the potential on diffusion rates have not yet been obtained. Clearly, ambipolarity requires long-term equality of ion and electron diffusion rates. This is not to be expected for heat transport, however, since a retaining potential has a strong influence on low-energy particles, whereas those of high energy are relatively unaffected. It is interesting to note that experimentally observed field fluctuation levels of $\delta B/B \approx 2 \times 10^{-5}$ may be large enough to make the electron diffusion (neglecting the potential) larger than the ion diffusion. Thus the magnitude and even the sign of the potential may depend on the fluctuation spectrum and level.

R.S. PEASE: Have you been able to calculate the bootstrap current as a function of the stochasticity?

R.B. WHITE: No, this has not yet been attempted. It is one of several interesting topics which we hope to pursue in the near future.